J. Cell. Mol. Med. Vol 14, No 9, 2010 pp. 2292-2304

Growth inhibition of colorectal carcinoma by lentiviral *TRAIL*-transgenic human mesenchymal stem cells requires their substantial intratumoral presence

Jana Luetzkendorf [#], Lutz P. Mueller [#, *], Thomas Mueller [#], Henrike Caysa, Katrin Nerger, Hans-Joachim Schmoll

Department of Internal Medicine IV, Oncology/Hematology, Martin-Luther-University Halle-Wittenberg, Halle, Germany

Received: January 19, 2009; Accepted: May 13, 2009

Abstract

Colorectal carcinoma (CRC) constitutes a common malignancy with limited therapeutic options in metastasized stages. Mesenchymal stem cells (MSC) home to tumours and may therefore serve as a novel therapeutic tool for intratumoral delivery of antineoplastic factors. Tumour necrosis factor (TNF)-related apoptosis inducing ligand (TRAIL) which promises apoptosis induction preferentially in tumour cells represents such a factor. We generated *TRAIL*-MSC by transduction of human MSC with a third generation lentiviral vector system and analysed their characteristics and capacity to inhibit CRC growth. (1) *TRAIL*-MSC showed stable transgene expression with neither changes in the defining MSC characteristics nor signs of malignant transformation. (2) Upon direct *in vitro* coculture *TR*AIL-MSC induced apoptosis in TRAIL-sensitive CRC-cell lines (DLD-1 and HCT-15) but also in CRC-cell lines resistant to soluble TRAIL (HCT-8 and SW480). (3) In mixed subcutaneous (s.c.) xenografts *TRAIL*-MSC inhibited CRC-tumour growth presumably by apoptosis induction but a substantial proportion of *TRAIL*-MSC within the total tumour cell number was needed to yield such anti-tumour effect. (4) Systemic application of *TRAIL*-MSC had no effect on the growth of s.c. DLD-1 xenografts which appeared to be due to a pulmonary entrapment and low rate of tumour integration of *TRAIL*-MSC. Systemic *TRAIL*-MSC caused no toxicity in this model. (5) Wild-type MSC seemed to exert a tumour growth-supporting effect in mixed s.c. DLD-1 xenografts. These novel results support the idea that lentiviral *TRAIL*-transgenic human MSC may serve as vehicles for clinical tumour therapy but also highlight the need for further investigations to improve tumour integration of transgenic MSC and to clarify a potential tumour-supporting effect by MSC.

Keywords: MSC • TRAIL • gene therapy • lentiviral • resistance • colorectal carcinoma

Introduction

Treatment options for metastasized colorectal carcinoma (CRC) after standard therapy are limited [1]. A promising new approach for an efficient tumour therapy comprises the use of stem cells as vehicles for the expression of tumour-inhibiting factors as in animal models an integration of stem cells into malignant tumours has been demonstrated [2–4]. A candidate for such an approach are mesenchymal stem cells (MSC) which can be easily obtained from adult tissues and are defined by standard criteria [5]. In xenograft models, transgenic MSC were shown to suppress tumour growth through ectopic expression of pro-apoptotic genes like interferon-β [6] or genes encoding enzymes activating antineoplastic prodrugs [7]. Specifically for CRC, such integration as well as an anti-tumour activity of transgenic MSC has been shown in animal models [7, 8].

The clinical application of transgenic MSC for tumour therapy requires (*i*) a transplantation approach without the need for subsequent immunosuppression; (*ii*) a safe and efficient expression of a transgene with high anti-tumour activity and little toxicity and (*iii*) an efficient and specific tumour integration of MSC.

The immunogenicity of MSC is a matter of debate [9] and an allogeneic setting still bears an undefined risk of rejection. We have previously shown that MSC can be derived from the bone marrow after extensive chemotherapeutic treatment [10]. Thus the

[#]These authors have contributed equally to this work.
*Correspondence to: Lutz P. MUELLER,
Department of Internal Medicine IV, Oncology/Hematology,
Martin-Luther-University Halle-Wittenberg,
Ernst-Grube-Str. 40, D-06120 Halle, Germany.
Tel.: +49-345-557 7278
Fax: +49-345-557 7279
E-mail: lutz.mueller@medizin.uni-halle.de

doi:10.1111/j.1582-4934.2009.00794.x

clinical use of autologous MSC from patients treated with chemotherapy is feasible and does not entail the risk of immunorejection.

A candidate for a potent anti-tumour transgene is Tumour necrosis factor (TNF)-related apoptosis-inducing ligand (TRAIL) which induces apoptosis through binding on death receptors (DR) leading to activation of the extrinsic apoptosis pathway *via* caspase-8. Generally, tumour cells show a higher sensitivity for TRAIL-induced apoptosis presumably due to a higher expression of death receptors in tumour cells and expression of decoy receptors in non-malignant cells [11]. Clinical trials with TRAIL or DR agonists are currently performed including patients with CRC [12]. However, *in vitro* studies demonstrate a resistance of some CRC-cell lines for soluble TRAIL-induced apoptosis [13, 14]. Aside from such resistance a low half-life of soluble TRAIL could hamper therapeutic applications as a permanent intratumoral presence of TRAIL would be favourable. As demonstrated by *in vitro* models *TRAIL*-transgenic progenitor or stem cells can exert a strong anti-tumour activity in adjacent tumour cells [15–18] and thus, the application of such cells could achieve a lasting intratumoral presence of TRAIL.

Transfection of MSC with bacterial plasmids results in a low frequency of stable genomic transgene insertion [19]. As *in vitro* cultured MSC populations may contain a considerable amount of quiescent cells [20], the use of lentiviral systems which allow an efficient genomic transgene integration even in quiescent cells seems favourable [21, 22].

Data on the effect of *TRAIL*-MSC on CRC cells *in vitro* and *in vivo* are missing. Starting from the observation of resistance of MSC to soluble TRAIL and the known TRAIL sensitivity of selected CRC-cell lines we generated human MSC expressing a lentiviral *TRAIL* construct and analysed their characteristics. *TRAIL*-MSC showed not only activity in TRAIL-sensitive CRC cells but also in two CRC-cell lines resistant to soluble TRAIL. We were able to show activity of *TRAIL*-MSC *in vivo*; nonetheless the activity of systemically applied *TRAIL*-MSC seemed to be hampered by their pulmonary entrapment. Our data suggest that a substantial amount of tumour-integrating *TRAIL*-MSC is required to exert a relevant anti-tumour activity. In addition our data suggest a tumour-supporting activity of wild-type MSC (WT-MSC). Therefore, our study supports the use of transgenic MSC for tumour therapy but also demonstrates the need for further studies before clinical applications can be ventured.

Material and methods

MSC, cell lines and cell culture

Cultivation as well as analysis of growth kinetics and differentiation of MSC isolated from human bone marrow according to a protocol approved by the institutional Ethics Board were performed as described previously [10] with the following modifications. Growth medium was composed of DMEM (low glucose, PAA, Pasching, Austria), 15% foetal calf serum (FCS) selected for optimal growth (Invitrogen, Grand Island, NY, USA) and 1% penicillin/streptomycin (PAA). For differentiation induction osteogenic medium (DMEM/10% FCS, 200 μM ascorbic acid 2-phosphate, 50 μM dexamethasone, 10 mM glycerol-3-phosphate) and adipogenic medium (DMEM/10% FCS, 10 μg/ml insulin, 100 μM indomethacin, 500 μM 3-isobutyl-1-methylxanthine, 50 μM dexamethasone, 5 μM rosiglitazone) (Sigma-Aldrich, St. Louis, MO, USA) were used. Treatment with soluble TRAIL was performed for 24 hrs with 100 ng/ml soluble *Killer*TRAIL (Axxora, San Diego, CA, USA) in growth medium. DiI (Invitrogen) labelling was performed at 2.5 μM in growth medium for 24 hrs immediately before transplantation.

The human CRC-cell lines HCT-8, HCT-15, DLD-1 and SW480 were cultivated in RPMI-1640 (PAA) with 10% FCS and 1% penicillin/streptomycin. Human embryonic kidney (HEK) 293T cells were cultivated in DMEM with 15% FCS and 1% penicillin/streptomycin.

Screening for TRAIL sensitivity of CRC-cell lines

Sensitivity of CRC-cell lines to soluble TRAIL was estimated by a sulforhodamine-B-assay according to established protocols [23]. CRC-cell lines were seeded at 5000 cells/well in three 96-well plates with eight wells per cell line on each plate, respectively. After 48 hrs one plate was fixed with 10% trichloroacetic acid ('control 0 hr'), one plate treated for 24 hrs with fresh growth medium ('control 24 hrs') and one plate treated with 100 ng/ml soluble *Killer*TRAIL for 24 hrs ('soluble TRAIL 24 hrs'). After 24 hrs the two treated plates were fixed with 10% trichloroacetic acid. Fixed plates were stained with 0.4% sulforhodamine-B (Sigma-Aldrich) as described [23]. Optical density (570 nm) was determined in a mircoplate reader and the mean of the eight wells for each cell line at the respective condition was calculated. Values from 'control 0 hr' were set 100% and compared to 'control 24 hrs' and 'soluble TRAIL 24 hrs'.

Plasmid constructs

Human *TRAIL*-cDNA was obtained from Jurkat-cell-RNA by RT-PCR using the primers 5′-AAGGAAGGGCTTCAGTGACC and 5′-AGTTAGCCAACTAAAAAGGCCC. The resulting cDNA covered bps 26–935 of human *TRAIL*-mRNA (NCBI accession no. U37518). *TRAIL*-cDNA was incorporated into pCR2.1-TOPO (Invitrogen), a *TRAIL*-containing *Eco*RI fragment was generated and the recessed ends were blunt-ended with Klenow enzyme.

From the transfer vector plasmid pFUGW [24] *GFP* was removed by *Bam*HI, *Eco*RI digestion. The recessed ends of the pFUGW backbone were blunt-ended and ligated with the blunt-ended *TRAIL* fragment. Insert direction and sequence fidelity of the resulting *TRAIL*-encoding transfer vector plasmid pFUTW were proven by sequencing.

DsRed-cDNA was obtained by PCR from pDsRed2-N1 (Clontech, Mountain View, CA, USA) with the primers 5′-GCCACCGGATCCACCATGGCCTCC and 5′-CCACCGAATTCTGGCTACAGGAA. The cDNA was cleaved with *Bam*HI and *Eco*RI and ligated into the *Bam*HI-*Eco*RI-fragment of pFUGW yielding the *DsRed*-encoding transfer vector plasmid pFUDW.

For lentiviral vector production the packaging plasmids pMDLg/pRRE and pRSV-Rev [22] and the envelope plasmid pVSVG were used. The plasmids pMDLg/pRRE, pRSV-Rev, pVSVG and pFUGW were kindly provided by Prof. Dr. T. Braun, Max-Planck-Institut für Herz- und Lungenforschung, Bad Nauheim.

Vector production and transduction of cells

Vector particles were produced by transient transfection of HEK293T cells with 10 μg transfer vector plasmid and 5 μg of pMDLg/pRRE, pRSV-Rev and pVSVG, respectively, by calcium phosphate DNA precipitation. After 48 hrs the vector containing supernatant was harvested, concentrated by ultracentrifugation and titred on HEK293T cells.

For transduction, cells were grown to 50% confluence and fed with fresh growth medium containing 8 μg/ml polybrene (Sigma-Aldrich). Transduction of MSC was performed at passage 1 or 2. Titres used for transduction were about 5×10^5 viral particles/ml. Medium was replaced after 24 hrs and the transgene expression was analysed after additional 24 hrs. Untransduced WT-MSC served as controls in the subsequent experiments.

Flow cytometry

Flow cytometry was performed as described previously [10]. MSC were labelled with the following mouse anti-human antibodies: Simultest Control γ_1/γ_1, anti-CD14-FITC, anti-CD45-PE, anti-HLA-DR-FITC, anti-CD19-PE, anti-CD34-FITC, anti-CD90-PE, anti-CD73-PE (BD Biosciences, Franklin Lakes, NJ, USA) and anti-CD105-FITC (Serotec, Oxford, UK).

For annexin V-staining the Annexin V-FITC Apoptosis detection kit I (BD Biosciences) was used according to manufacturer's instructions. All analyses were performed on a FACSCalibur using CellQuest software (all BD Biosciences).

Immunocytochemistry

Cells were cultivated in chamber slides and fixed with methanol/acetone (1:1) or 2% formalin. The primary mouse antibodies – control IgG1 (Ancell Corporation, Bayport, MN, USA), anti-TRAIL clone 2E5 (Axxora) on methanol/acetone-fixed slides and anti-TRAIL clone ZZ02 (Santa Cruz Biotechnology, Santa Cruz, CA, USA) on formalin-fixed slides – were used at 10 μg/ml over night. After washing, slides were incubated with 5 μg/ml IRDye680-conjugated goat antimouse IgG (LI-COR Biosciences, Lincoln, NE, USA) for 1 hr. Subsequently, slides were exposed to 1 μg/ml DAPI (Sigma-Aldrich) for counterstaining of nuclei, covered with fluorescence mounting medium and analysed on a Nikon Eclipse TE2000-E (Nikon, Düsseldorf, Germany). All procedures were performed at room temperature.

Coculture experiments

TRAIL-MSC or WT-MSC (10,000 cells/cm^2, respectively) were mixed with *DsRed*-DLD-1 cells (50,000 cells/cm^2) or *DsRed*-HCT-8 cells (60,000 cells/cm^2) and plated in 12-well plates. After 24 hrs detached cells were harvested, counted and analysed for annexin V-staining. Adherent cells from one well were harvested, counted and analysed by flow cytometry for DsRed expression. This procedure was repeated 48 hrs and 72 hrs after initial plating. The TRAIL-neutralizing antibody (clone 2E5) was used at a concentration of 10 μg/ml.

Lysates of whole coculture (*i.e.* all adherent and detached cells) and lysates from detached cells only were prepared from separate wells after 24 hrs cocultivation of CRC cells (DLD-1 50,000 cells/cm^2, HCT-8 60,000 cells/cm^2, HCT-15 and SW480 each 100,000 cells/cm^2) with WT-MSC and with *TRAIL*-MSC (each 10,000 cells/cm^2), respectively.

Western blotting

Western blot analyses were performed as described previously [10] using the following primary mouse antibodies: anti-caspase-3 (0.5 μg/ml, MBL, Woburn, MA, USA), anti-caspase-8 (0.5 μg/ml, Invitrogen), anti-poly (ADP-ribose) polymerase (PARP) (1 μg/ml, BD Biosciences), anti-TRAIL (0.5 μg/ml, clone HS501, Axxora) and anti-tubulin (0.1 μg/ml, Dianova, Hamburg, Germany). Immunocomplexes were visualized by enhanced chemiluminescence (Amersham Pharmacia Biotech, Little Chalfont, England) using horseradish peroxidase-conjugated antimouse IgG (0.1 μg/ml, Santa Cruz Biotechnology) and Roti-Lumin (Carl Roth, Karlsruhe, Germany).

Animal studies

Six- to 8-week-old athymic nude-fox n1 nu/nu mice (Harlan Winkelmann, Borchen, Germany) were used for the *in vivo* experiments according to institutional guidelines under approved protocols.

Subcutaneous (s.c.) mixed xenografts were generated as follows: 3×10^6 *DsRed*-CRC cells per tumour were mixed with *TRAIL*-MSC or with control MSC (*GFP*- or WT-MSC) and administered into the right (*TRAIL*-MSC) and the left (control MSC) flank of one animal. The following proportions of MSC were used in mixed xenografts: 7.5×10^5 (*i.e.* 20% of total injected cell number), 3.33×10^5 (10%), 9.3×10^4 (3%) and 3.03×10^4 (1%). Tumour growth was determined over 17 days by fluorescence imaging. Animals were killed and dissected tumours were embedded in paraffin.

For studying the effects of systemically applied MSC 5×10^6 *GFP*-DLD-1 cells were injected s.c. into the left flank of one animal. 2.25×10^5 DiI-labelled *TRAIL*- (treatment) or WT-MSC (cell control) or a respective volume of PBS (control) were administered into tail vein after 2, 4, 7, 10 and 15 days. Tumour growth was determined over 18 days by fluorescence imaging. After killing of animals, lungs and s.c. tumours were dissected and cryosections were prepared.

Every experiment was done at least in triplicates. None of the animals had to be killed prematurely due to tumour burden or impaired vital parameters.

Image acquisition and analysis

A 2.2 CRi Maestro *in vivo* fluorescence imaging system (CRi, Woburn, MA, USA) was used to acquire multispectral images. DsRed-expressing tumours were imaged using the green filter set (excitation 503 to 550 nm, emission 580 nm longpass). Acquisition settings were 550 to 800 nm in 10-nm steps. GFP-expressing tumours were imaged using the blue filter set (excitation 445 to 490 nm, emission 515 nm longpass). Acquisition settings were 500 to 720 nm in 10-nm steps. Exposure time was set automatically.

Determination of fluorescence signals was performed with Maestro software (2.22). For quantification a region of interest around the s.c. tumour was analysed by setting threshold as zero. The total signal intensity was divided by exposure time to allow comparison.

Immunohistochemistry

Immunohistochemical staining of paraffin slides was performed as described previously [25]. The following antibodies were used at room temperature: rabbit anti-PARP-1 (Cleaved p25, Epitomics, Burlingame, CA,

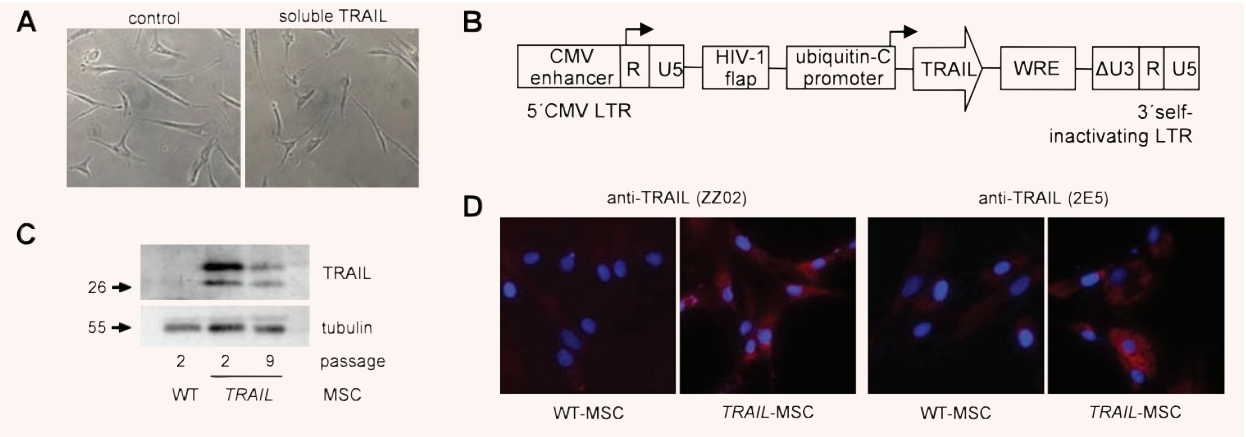

Fig. 1 Resistance of MSC to soluble TRAIL and stable expression of TRAIL at the cell surface of MSC upon lentiviral transduction. (**A**) MSC were treated for 24 hrs with 100 ng/ml soluble TRAIL in growth medium. Control cells were cultivated in growth medium. Light microscopy, original magnification ×100. (**B**) Diagram of the lentiviral vector FUTW used to generate *TRAIL*-MSC. Only the relevant portions of the plasmid are shown. (**C**) MSC were transduced with FUTW at passage 1. Whole protein lysates from WT-MSC and *TRAIL*-MSC were analysed by Western blot for expression of the transmembraneous form of the TRAIL protein (34 kD). Tubulin (55 kD) served as control for equal protein loading. Arrows indicate the respective molecular weight standards in kD. (**D**) WT-MSC and *TRAIL*-MSC were fixed on chamber slides and stained with mouse anti-TRAIL (clone ZZ02 and 2E5) and IRDye680 goat antimouse IgG (red). Nuclei were counter-stained with DAPI (blue). Slides were analysed on a Nikon Eclipse TE2000-E. Images are shown as overlays of antibody and DAPI fluorescence. Fluorescence microscopy, original magnification ×600.

USA) at a dilution of 1:2000 for 3 hrs, biotin-labelled anti-rabbit IgG and HRP-conjugated streptavidine both at 0.5 μg/ml for 1 hr (Santa Cruz Biotechnology). Immunocomplexes were visualized with 3,3′-diaminobenzidine; slides were counterstained with haematoxyline and mounted with DePeX (all Dako, Glostrup, Denmark).

Statistical analysis

Statistical analysis was performed with SPSS 14.0 software (SPSS Inc. Chicago, IL, USA). An updated t-test including Levene testing for variances was used. A *P*-value <0.05 was considered significant.

Results

Stable expression of TRAIL at the cell surface of MSC upon lentiviral transduction

Human MSC showed no morphological signs of apoptosis induction upon treatment with soluble TRAIL for 24 hrs, particularly no detachment of cells (Fig. 1A) and also no staining with annexin V (data not shown). We concluded that TRAIL could serve as a factor to be expressed in MSC in order to mediate an anti-tumour effect by tumour-integrating *TRAIL*-transgenic MSC.

TRAIL-MSC were generated through lentiviral transduction of MSC (for lentiviral construct see Fig. 1B). Western blot analyses of whole protein lysates revealed TRAIL expression at the size of the membrane bound protein (34 kD) over up to nine passages (Fig. 1C). Immunocytochemical analysis with two different antibodies raised against an extracellular domain of human TRAIL indicated presence of TRAIL at the cell surface (Fig. 1D). Incubation with control mouse IgG1 did not result in detectable staining (data not shown) and no TRAIL expression could be detected in WT-MSC (Fig. 1C, D). At passage 4 after transduction approximately 80% of the cells showed TRAIL expression in immunocytochemical analysis (data not shown).

Thus, lentiviral transduction of human MSC with *TRAIL* yielded an efficient and stable transgene expression with localization of TRAIL at the cell surface. Next we wanted to investigate whether lentiviral *TRAIL* expression altered the defining properties of MSC.

Unaltered MSC characteristics in *TRAIL*-MSC

We analysed *TRAIL*-MSC for their MSC characteristics as defined by consensus criteria [5]. Flow cytometric analyses revealed an identical immunophenotype for *TRAIL*-MSC and WT-MSC, *i.e.* $CD14^-$, $CD19^-$, $CD34^-$, $CD45^-$, $HLA\text{-}DR^-$, $CD73^+$, $CD90^+$, $CD105^+$ (Fig. 2A) and glycophorin-A^-, $CD11c^-$, $CD13^+$, $CD29^+$, $CD44^+$, $CD166^+$ (data not shown). Following adipogenic and osteogenic differentiation induction, *TRAIL*-MSC showed multipotent differentiation with intracellular accumulation of lipid droplets and calcium deposition, respectively (Fig. 2B).

Conclusively, transgenic *TRAIL* expression in human MSC did not alter their defining MSC characteristics in comparison to

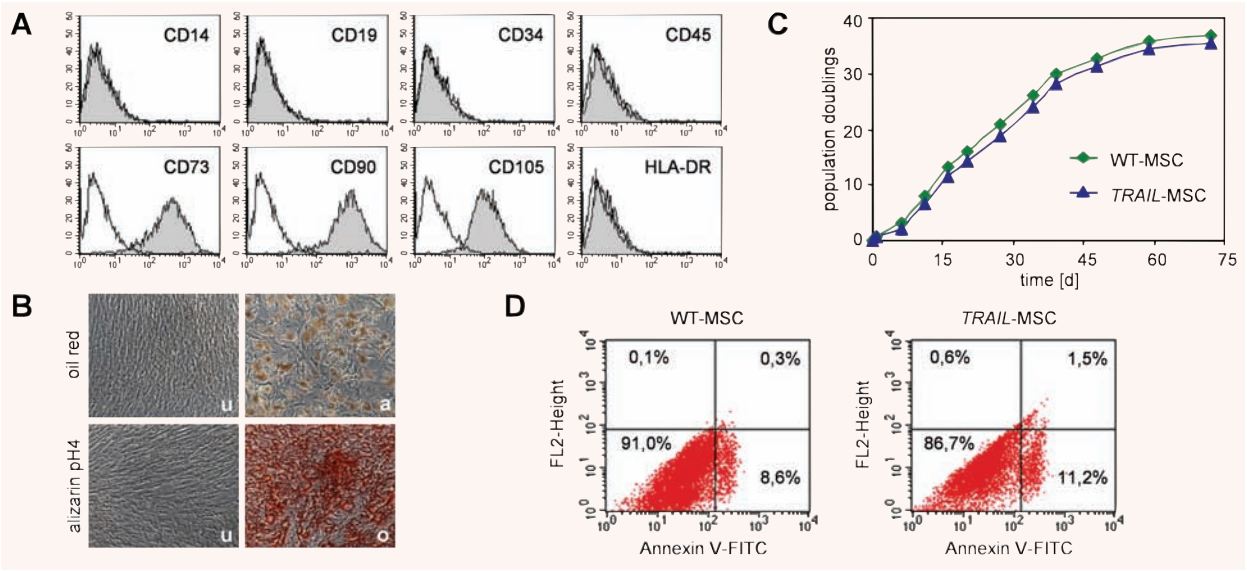

Fig. 2 Neither alterations in defining MSC characteristics nor signs of malignant transformation due to lentiviral TRAIL-expression. (**A**) *TRAIL*-MSC were analysed for surface antigen expression by flow cytometry. Data are shown as histograms of fluorescence. Isotype controls (no filling) are overlaid on specific FITC- or PE-conjugated antibodies. Representative data of one experiment out of seven are presented. (**B**) *TRAIL*-MSC were incubated in growth medium (u) or specific osteogenic (o) and adipogenic (a) differentiation media. Cells were stained with alizarin pH4 and oil red for calcium deposition and lipid droplets, respectively. Data are representative of five independent experiments. Light microscopy, original magnification ×100. (**C**) Growth kinetic was performed with WT-MSC (green square) and *TRAIL*-MSC (blue triangle) from the same donor. Transduction was performed on day 0. Proliferation was analysed by seeding the cells with 200/cm^2 and subsequent passaging and cell counting at 50–60% confluence for 11 passages. Population doubling (PD) was calculated. Data are representative of nine independent experiments. (**D**) WT-MSC and *TRAIL*-MSC were cultivated over five passages, stained with annexin V-FITC and analysed by flow cytometry.

WT-MSC. As lentiviral transduction poses the risk of oncogene activation we analysed signs of malignant transformation in *TRAIL*-MSC.

Lack of malignant transformation of *TRAIL*-MSC

To assess the potential of malignant transformation of *TRAIL*-MSC we performed growth kinetics, soft agar assays and karyotype analysis with *TRAIL*-MSC and untransduced WT-MSC from the same donor starting at the time of transduction. *TRAIL*-MSC showed no changes in proliferation kinetics compared to WT-MSC (Fig. 2C). Neither soft agar colony formation nor karyotypic changes were observed in *TRAIL*–MSC (data not shown).

The transgenic expression of TRAIL may lead to apoptosis induction in transduced cells. However, we observed no increased annexin V-staining in *TRAIL*-MSC when compared to WT-MSC (Fig. 2D), indicating that transgenic TRAIL did not mediate apoptosis induction in *TRAIL*-MSC. These data were in accordance with the observed similar proliferation of *TRAIL*-MSC and WT-MSC (Fig. 2C).

Thus, lentiviral expression of *TRAIL* did neither result in signs of malignant transformation nor in apoptosis induction in human MSC. These data suggested that *TRAIL*-MSC may serve as a vehicle for tumour growth inhibition and we aimed to investigate their effect on TRAIL-sensitive CRC cells *in vitro*.

Apoptosis induction in TRAIL-sensitive CRC cells through *TRAIL*-MSC *in vitro*

As the CRC-cell line DLD-1 is reportedly sensitive to soluble TRAIL [26], we performed the initial analysis of the tumour-inhibiting capacity of *TRAIL*-MSC in this cell line. *DsRed*-DLD-1 cells were exposed to either *TRAIL*-MSC or WT-MSC in direct cocultures over 24 hrs *in vitro*. Occurrence of detached cells suggesting apoptosis was observed in cocultures with *TRAIL*-MSC but not with WT-MSC. These detached cells originated from DLD-1 cells, as shown by their DsRed expression (Fig. 3A). When cocultures containing *TRAIL*-MSC were supplemented with TRAIL-neutralizing antibody, no cell detachment was observed (Fig. 3A). Direct cell–cell contact was necessary for induction of detachment, as no relevant detachment of cells occurred upon incubation of DLD-1 cells with conditioned medium from *TRAIL*-MSC cultures (data not shown).

Proliferation of the respective cell subpopulations was assessed by determining the total cell numbers and the proportion of DsRed$^+$ cells. In direct coculture with *TRAIL*-MSC over up to

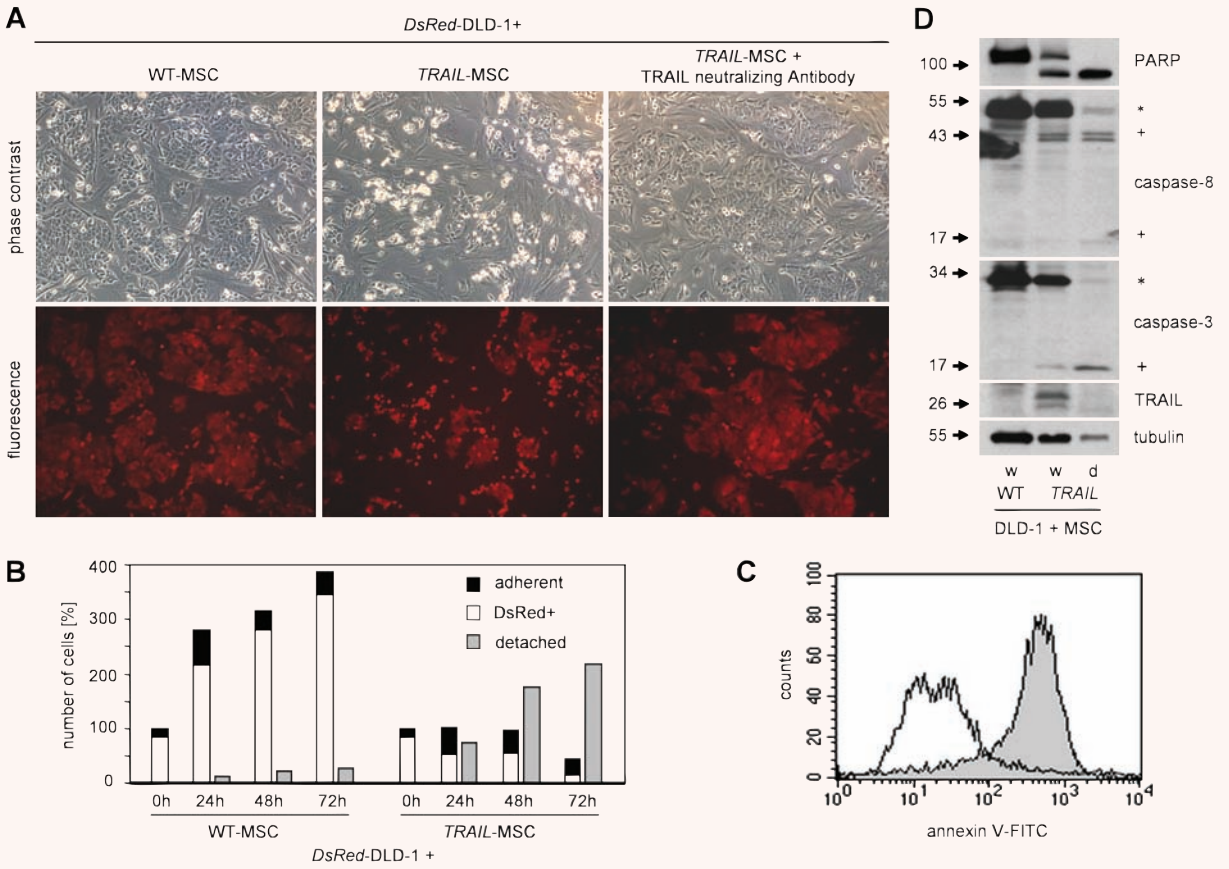

Fig. 3 Apoptosis induction in TRAIL-sensitive CRC cells through *TRAIL*-MSC *in vitro*. (**A**) *DsRed*-DLD-1 cells were cocultivated with WT- and *TRAIL*-MSC, respectively, for 24 hrs. For the experiment depicted in the far right panel 10 μg/ml TRAIL-neutralizing antibody was supplemented. Light microscopy, original magnification ×100. In the lower panel the respective fluorescence images are pictured. (**B**) *DsRed*-DLD-1 cells were cocultivated with WT- and *TRAIL*-MSC, respectively. At the indicated time-points the number of detached cells (grey bars) as well as the proportion of DsRed$^+$ DLD-1 cells (white bars) within the total number of adherent cells (black bars) was determined. For comparison, cell numbers at start of coculture (0 hr) were set as 100%. Data are representative of four independent experiments. (**C**) Detached cells after 24 hrs coculture with *TRAIL*-MSC from experiment in (**B**) were stained with annexin V-FITC (grey filling) and analysed by flow cytometry. Untreated *DsRed*-DLD-1 cells were stained as controls (no filling). Data are shown as histograms of fluorescence. (**D**) Lysates from direct cocultures after 24 hrs were obtained as whole (w) lysates, *i.e.* all adherent and detached cells combined as well as detached cell (d) lysates from an additional coculture with *TRAIL*-MSC and subsequently analysed by Western blot. Tubulin served as a loading control. Arrows indicate the respective molecular weight standards in kD. '*' indicates the procaspases and '+' the cleaved fragments. Data are representative of three independent experiments.

72 hrs the absolute number of *DsRed*-DLD-1 cells decreased when compared to initially plated cell numbers. In contrast, a continuous increase of *DsRed*-DLD-1 cell numbers was seen in cocultures with WT-MSC. The number of detached DsRed$^+$ DLD-1 cells increased only in direct coculture with *TRAIL*-MSC (Fig. 3B).

As DLD-1 cells did not express CD105 (data not shown) we examined CD105 expression on adherent cells to exclude cell fusion as a relevant contribution to the number of adherent DsRed$^+$ cells. However adherent cells positive for CD105 showed no DsRed expression, *i.e.* uptake of DsRed by MSC did not skew the results (data not shown).

Cocultures with *TRAIL*-MSC resulted in apoptosis induction in DLD-1 cells since the detached cells stained positive with annexin V (Fig. 3C). This involved activation of the entire extrinsic apoptosis pathway since cleavage of PARP (116 kD), yielding an 85-kD fragment as well as cleavage of procaspase-8 (55 kD) and procaspase-3 (32 kD) into their active fragments of caspase-8 (41 and 18 kD) and caspase-3 (17 kD) was observed in cocultures of *DsRed*-DLD-1 with *TRAIL*-MSC. Cleavage of PARP and caspases was most prominent in detached cells (Fig. 3D). Apoptosis occurred solely in DLD-1 cells as detached cells were DsRed$^+$ (Fig. 3A) and showed no expression of TRAIL (Fig. 3D). Induction

of apoptosis depended on the presence of *TRAIL*-MSC as in cocultures of *DsRed*-DLD-1 cells with WT-MSC neither relevant amounts of detached cells occurred (Fig. 3A) nor cleavage of PARP and procaspases was observed (Fig. 3D).

Taken together, these data showed first, that TRAIL is functionally expressed in lentivirally transduced human MSC. Secondly, upon direct coculture, *TRAIL*-MSC induced apoptosis in TRAIL-sensitive DLD-1 cells resulting in a reduction of total tumour cell number. We suggested that direct interaction with ectopically *TRAIL*-expressing MSC may overcome TRAIL-resistance in CRC cells.

Apoptosis induction in TRAIL-resistant CRC cells through *TRAIL*-MSC *in vitro*

Next, we aimed to assess the anti-tumour activity of *TRAIL*-MSC in other CRC-cell lines. At first we analysed the response to soluble TRAIL in four CRC-cell lines *in vitro*. Upon TRAIL treatment, a reduction in the cell number below the pre-treatment values was observed for the cell lines HCT-15 and DLD-1. They were thus determined to be TRAIL-sensitive (Fig. 4A-a). The cell lines SW480 and HCT-8 showed continued cell proliferation upon TRAIL treatment and were therefore determined to be TRAIL-resistant (Fig. 4A-a). Growth inhibition occurred to some degree in TRAIL-resistant CRC-cells lines as demonstrated by the reduced cell numbers in comparison to the respective untreated controls at 24 hrs (Fig. 4A-a).

Subsequently, all four CRC-cells lines were directly cocultured with either WT-MSC or *TRAIL*-MSC. Western blot analyses revealed apoptosis induction as indicated by cleavage of PARP in TRAIL-sensitive CRC-cell lines as well as in the TRAIL-resistant CRC-cells lines SW480 and HCT-8 (Fig 4A-b).

The response to *TRAIL*-MSC was further investigated in the TRAIL-resistant HCT-8 cell line. $DsRed^+$ detached cells were observed after 24 hrs coculture of *DsRed*-HCT-8 cells with *TRAIL*-MSC but not in cocultures with WT-MSC (Fig. 4B). As for DLD-1 cells, detachment of $DsRed^+$ cells was inhibited by a TRAIL-neutralizing antibody (Fig. 4B) and required direct cell–cell contact as no relevant detachment of HCT-8 cells occurred upon incubation with *TRAIL*-MSC conditioned medium (data not shown).

Coculture with *TRAIL*-MSC abolished the expansion of *DsRed*-HCT-8 cells although in contrast to DLD-1 cells the number of tumour cells at 72 hrs was not reduced in comparison to the initially plated cell numbers (Fig. 4C). The number of detached cells increased over the whole period in coculture with *TRAIL*-MSC while coculture with WT-MSC resulted in a rapid growth of *DsRed*-HCT-8 cells without detachment of cells (Fig. 4C). In cocultures with *TRAIL*-MSC detached cells stained with annexin V and cleavage of PARP, procaspase-8 and procaspase-3 was observed (Fig. 4D, E), supporting the notion of *TRAIL*-MSC induced apoptosis in HCT-8 cells. Detached cells were positive for DsRed indicating an exclusive induction of apoptosis in CRC cells (Fig. 4B). However, Western blot analysis of the detached cells showed a weak signal for TRAIL (Fig. 4E). As Ponceau S staining revealed equal protein loading for lysates of whole culture and detached cells we conclude that the faint TRAIL signal in detached cells indeed represented a very low level of TRAIL protein. The weaker signal for tubulin in detached cells in Fig. 4E despite equal protein loading can be explained by the reported [27] degradation of tubulin upon apoptosis. Conclusively, the very low level of TRAIL protein in lysates of detached cells could reflect a low degree of detachment of *TRAIL*-MSC as a bystander effect of apoptosis induction in adjacent HCT-8 cells. However, this low extent of detachment of *TRAIL*-MSC upon coculture with HCT-8 cells does apparently not interfere with the efficacy of apoptosis induction by *TRAIL*-MSC. As for DLD-1 cells, in cocultures of HCT-8 cells with WT-MSC no cleavage of PARP and procaspases was observed (Fig. 4E).

Thus, upon direct cell–cell contact *in vitro*, *TRAIL*-MSC are capable to induce apoptosis and to inhibit tumour cell growth not only in TRAIL-sensitive CRC-cell lines but also in two CRC-cell lines with proven resistance to soluble TRAIL. We therefore assumed that *TRAIL*-MSC may be capable of inhibiting tumour growth *in vivo*.

Reduction of tumour growth involving apoptosis induction by *TRAIL*-MSC *in vivo*

We generated s.c. xenografts of *DsRed*-DLD-1 cells mixed 4:1 with either *TRAIL*-MSC, *GFP*-MSC or WT-MSC, *i.e.* MSC amounting a proportion of 20% of the entire injected cell number. Tumour size was examined by *in vivo* fluorescence imaging of DsRed fluorescence intensity. After an identical decrease in fluorescence intensity until day 5 the signal intensities from DLD-1 xenografts mixed with *GFP*-MSC increased whereas intensities from xenografts with *TRAIL*-MSC remained low (Fig. 5A, B). This reflected a significant growth inhibition of DLD-1 xenografts by *TRAIL*-MSC compared to *GFP*-MSC ($P = 0.006$; confidence interval 350.3–1128.5) (Fig. 5B) and to WT-MSC (data not shown). A similar difference in tumour growth between xenografts containing WT-MSC and *TRAIL*-MSC containing xenografts was observed when size and weight of dissected tumours were compared (data not shown).

Next, we generated s.c. xenografts of the TRAIL-resistant *DsRed*-HCT-8 cell line mixed 4 : 1 with either *TRAIL*-MSC or WT-MSC. As measured by *in-vivo* imaging, HCT-8 xenografts containing *TRAIL*-MSC showed reduced growth compared to HCT-8 xenografts containing WT-MSC (Fig. 5C). Similar results were obtained when weight of dissected tumours were compared (data not shown). Thus, tumour-integrated *TRAIL*-MSC mediated inhibition of tumour growth not only in xenografts from TRAIL-sensitive DLD-1 cells but also in xenografts from TRAIL-resistant HCT-8 cells.

To prove apoptosis induction as the cause for reduced tumour growth we generated xenografts of *DsRed*-DLD-1 cells mixed with *TRAIL*-MSC in a proportion of 33:1, *i.e. TRAIL*-MSC comprising

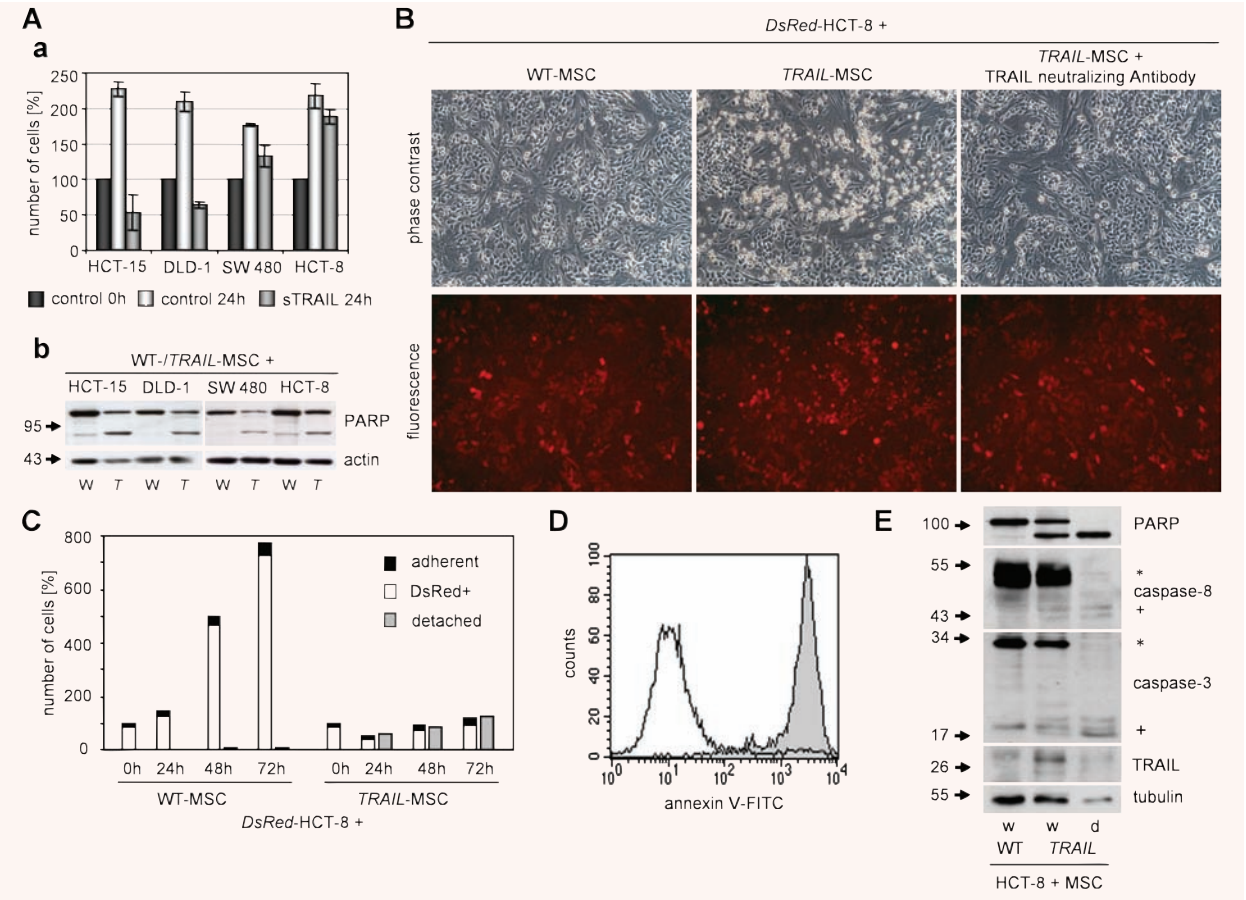

Fig. 4 Apoptosis induction in TRAIL-resistant CRC cells through *TRAIL*-MSC *in vitro*. (**A**) (a) Growing CRC-cell lines were treated for 24 hrs with growth medium (control 24 hrs; white bars) or soluble TRAIL (sTRAIL 24 hrs; grey bars), cell numbers were estimated by a sulforhodamine-B-assay and compared to untreated controls (control 0 hr; black bars). Data are shown as mean ± standard deviation of two independent experiments. (b) CRC-cell lines were cultivated in direct coculture with WT-MSC (W) and *TRAIL*-MSC (T) for 24 hrs. Whole cell lysates were harvested and analysed by Western blot for cleavage of PARP. Actin served as loading control. Arrows indicate the respective molecular weight standards in kD. (**B**) *DsRed*-HCT-8 cells were cultivated in direct coculture with WT- and *TRAIL*-MSC for 24 hrs. In the far right panel the medium was supplemented with 10 μg/ml TRAIL-neutralizing antibody. Light microscopy, original magnification ×100. In the lower panel the respective fluorescence images are pictured. (**C**) *DsRed*-HCT-8 cells were cocultivated with WT- and *TRAIL*-MSC, respectively. At the indicated time-points the number of detached cells (grey bars) as well as the proportion of $DsRed^+$ HCT-8 cells (white bars) within the total number of adherent cells (black bars) were determined. For comparison, cell numbers at start of coculture (0 hr) were set as 100%. Data are representative of two independent experiments. (**D**) Detached cells after 48 hrs from (**C**) were stained with annexin V-FITC (grey filling) and analysed by flow cytometry. As control served untreated *DsRed*-HCT-8 cells stained with annexin V-FITC (no filling). Data are shown as histograms of fluorescence. (**E**) Lysates from direct cocultures after 24 hrs were obtained as whole (w) lysates, *i.e.* all adherent and detached cells combined as well as detached cell (d) lysates from an additional coculture with *TRAIL*-MSC and subsequently analysed by Western blot. Tubulin served as loading control. Arrows indicate the respective molecular weight standards in kD. '*' indicates the procaspases and '+' the cleaved fragments. Data are representative of two independent experiments.

3% of total cell number injected. This lower proportion was used since the lack of tumour growth with 20% *TRAIL*-MSC rendered histological examination impossible. A relevant tumour size was reached not earlier than day 7 and tumours were dissected on day 9. Histochemistry showed staining for cleaved PARP near stromal elements within the tumour (Fig. 5D) indicative for *TRAIL*-MSC induced apoptosis in CRC cells.

We concluded first, that human MSC retained functional expression of lentiviral *TRAIL in vivo* and second, that *TRAIL*-MSC can reduce tumour growth of CRC cells *in vivo* through induction of apoptosis. Given the published data on integration of MSC into tumours we next wanted to investigate the effect of systemically transplanted *TRAIL*-MSC on the growth of CRC xenografts.

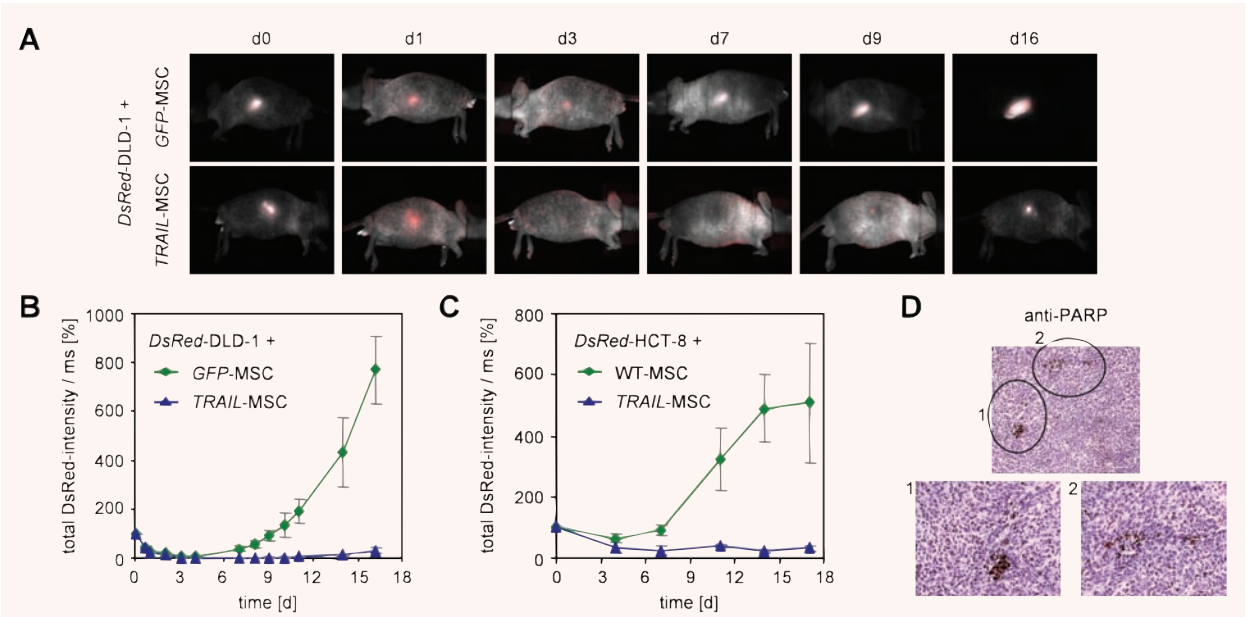

Fig. 5 Reduction of tumour growth involving apoptosis induction by *TRAIL*-MSC *in vivo* (**A**) *DsRed*-DLD-1 cells were mixed with *GFP*-MSC or *TRAIL*-MSC at a proportion of 4:1 (*i.e.* 20% MSC of total cell number injected) and injected in nude mice subcutaneously into the left or right flank, respectively, at day 0. Tumour size on both sides of each animal was examined by imaging the fluorescence intensity of the DsRed signal. Exposure time was set automatically. A representative range of images from one mouse out of three experiments is pictured. (**B**) DsRed-fluorescence intensities of xenografts from *DsRed*-DLD-1 cells mixed with 20% *GFP*-MSC (green square) or 20% *TRAIL*-MSC (blue triangle) as described under (**A**) were quantified. The total DsRed-signal intensity of tumours divided by exposure time in ms is plotted. The total intensity / ms 2.5 hrs after generating xenografts was set as 100%. Data are depicted as mean ± standard error of the mean ($N = 3$). (**C**) *DsRed*-HCT-8 cells were mixed with WT-MSC (green square) or *TRAIL*-MSC (blue triangle) at a proportion of 4 : 1 (*i.e.* 20% MSC of total cell number injected) and injected in nude mice subcutaneously into the left or right flank, respectively, at day 0. Tumour size on both sides of each animal was examined by imaging the fluorescence intensity of the DsRed-signal. DsRed-fluorescence intensities of mixed xenografts were quantified. The total DsRed-signal intensity of tumours divided by exposure time in ms is plotted. The total intensity / ms 3 hrs after generating xenografts was set as 100%. Data are depicted as mean ± standard error of the mean ($N = 3$). (**D**) Histochemical staining with an antibody against the 25 kD fragment of cleaved PARP in paraffin-embedded sections of a mixed xenograft generated with *DsRed*-DLD-1 cells mixed with 3% *TRAIL*-MSC. Antibody binding was visualized with diaminobenzidine (brown staining). Slides were counterstained with haematoxyline. Light microscopy, original magnification ×100 and ×400.

Lack of effects of systemic *TRAIL*-MSC on growth of s.c. CRC xenografts

DiI-labelled *TRAIL*- or WT-MSC were injected into the tail vein in mice bearing s.c. *GFP*-DLD-1 xenografts. Tumour size was examined by *in vivo* fluorescence imaging.

In comparison to controls receiving no MSC a similar tumour growth occurred in mice receiving WT-MSC as well as in mice receiving *TRAIL*-MSC (Fig. 6A). No signs of toxicity were seen upon systemic transplantation of *TRAIL*-MSC. In particular no organ dysfunction and no formation of additional tumours were observed upon live observation of animals and macroscopic inspection after killing.

Ex vivo fluorescence imaging of whole dissected lungs showed strong signals in accordance with a pulmonary entrapment of the applied MSC (Fig. 6B). Lungs from animals which received no MSC (Fig. 6B) as well as dissected s.c. tumours from all animals showed no signals in whole organ fluorescence imaging (data not shown). In cryosections of lungs from animals which received DiI-labelled *TRAIL*-MSC we saw large areas of red fluorescent cells confirming a pulmonary accumulation of MSC. Cryosection of s.c. tumours from these animals showed only a few DiI signals (Fig. 6C), indicating that only a very low percentage of MSC had integrated into s.c. tumours representing approx. 0.1% of total tumour cells.

We presumed that the lack of effects of systemic *TRAIL*-MSC on CRC growth was due to the low rate of tumour integration of *TRAIL*-MSC as a consequence of their pulmonary entrapment. To clarify this observation we evaluated the amount of tumour-integrated *TRAIL*-MSC required to inhibit tumour growth in our s.c. CRC-xenograft model.

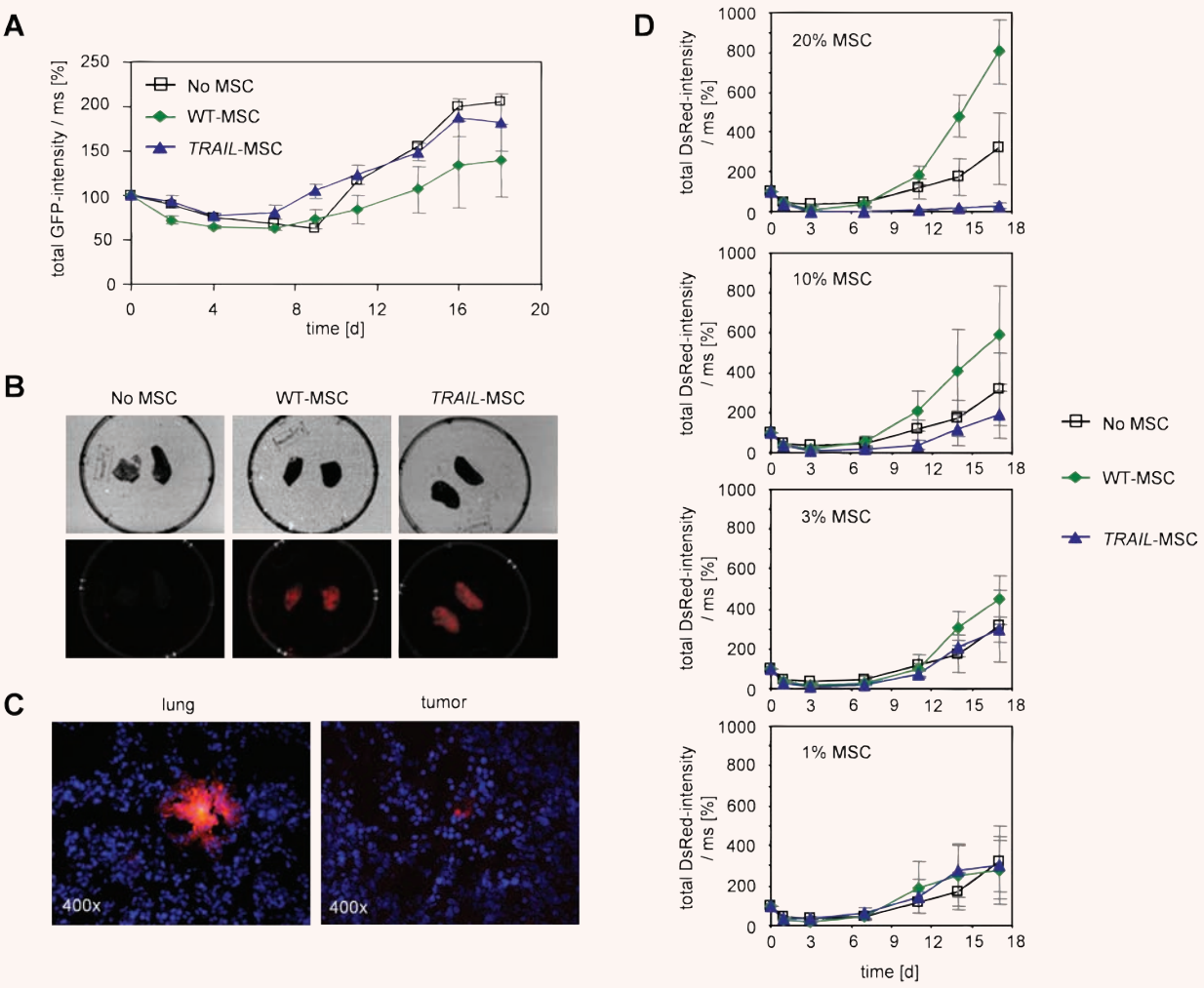

Fig. 6 Lack of effects of systemic *TRAIL*-MSC on growth of s.c. CRC xenografts due to poor tumour integration in agreement with the need for a substantial proportion of tumour-integrated *TRAIL*-MSC to inhibit CRC-tumour growth *in vivo*. (**A**) DiI-labelled WT- and *TRAIL*-MSC were injected into tail vein of nude mice bearing s.c. *GFP*-DLD-1 xenografts on days 2, 4, 7, 10 and 15. Tumour sizes were quantified by imaging the GFP-fluorescence intensity of xenografts without MSC application (black square), with i.v. WT-MSC (green square) and with i.v. *TRAIL*-MSC (blue triangle). The total GFP-signal intensity divided by exposure time in ms is plotted. The total intensity / ms 2.5 hrs after generating xenografts was set 100%. Depicted as mean ± standard error of the mean ($N = 3$), except for tumours without MSC application ($N = 1$). (**B**) Lungs from mice with and without i.v. application of DiI-labelled WT- or *TRAIL*-MSC were dissected and imaged *ex vivo* to visualize DiI-labelled cells (red). The upper panel shows greyscale images. In the lower panel the respective fluorescence images are pictured. (**C**) Cryosections from lung and s.c. DLD-1 xenograft after i.v. application of DiI-labelled *TRAIL*-MSC. Nuclei were counterstained with DAPI. Fluorescence images are pictured as overlays of DiI (red) and DAPI (blue) fluorescence. Original magnification ×400. (**D**) S.c. mixed xenografts were generated with *DsRed*-DLD-1 cells and different amounts of WT-MSC (i.e. native or *GFP*-MSC) or *TRAIL*-MSC. Tumour size was examined by imaging the DsRed fluorescence intensity. Fluorescence signals of xenografts from *DsRed*-DLD-1 cells without MSC (black square), from *DsRed*-DLD-1 cells mixed with WT-MSC (green square) and *TRAIL*-MSC (blue triangle) were quantified. The total DsRed-signal intensity of tumours divided by exposure time in ms is plotted. The total intensity / ms 2.5 hrs after generating xenografts was set as 100%. Depicted as mean ± standard error of the mean (20% MSC $N = 9$; 10% $N = 6$; 3% $N = 6$; 1% $N = 3$; no MSC $N = 4$). Statistical relevance is only reached in comparison of 20% *TRAIL*-MSC with 20% WT-MSC ($P = 0.005$). Note that for 20% MSC the curve for WT-MSC is composed of data from xenografts with 20% *GFP*-MSC ($N = 6$) and with 20% WT-MSC ($N = 3$).

Requirement for a substantial proportion of tumour-integrated *TRAIL*-MSC to inhibit CRC-tumour growth *in vivo*

We generated s.c. mixed xenografts of *DsRed*-DLD-1 with different proportions of either WT-MSC (*i.e.* native or *GFP*-MSC) or *TRAIL*-MSC. Tumour size was examined by *in vivo* fluorescence imaging of tumour derived DsRed-signal and tumour size at the end of the experiment (day 17) was statistically compared.

Compared to xenografts without MSC, a proportion of 20% *TRAIL*-MSC reduced the tumour size considerably although this difference did not reach significance given the high standard deviations ($P = 0.21$; confidence interval –861.2 to 286.0). With 10% *TRAIL*-MSC the tumour growth inhibition was less pronounced ($P = 0.6$) and 3% or 1% *TRAIL*-MSC had no effect on tumour growth ($P = 0.9$) in comparison to xenografts without MSC (Fig. 6D).

However, when the size of xenografts containing *TRAIL*-MSC were compared to xenografts containing WT-MSC (Fig. 6D) a significant difference was observed for 20% *TRAIL*-MSC *versus* 20% WT-MSC ($P = 0.005$; confidence interval 359.2–1190.9) and a still obvious difference for 10% *TRAIL*-MSC *versus* 10% WT-MSC ($P = 0.18$; confidence interval –214.5 to 1015.6) was seen.

This observation suggested that WT-MSC supported the growth of s.c. DLD-1 xenografts. Compared to xenografts without MSC, 20% WT-MSC increased tumour size at the end of the experiment considerably ($P = 0.085$; confidence interval –83.8 to 1058.7). A facilitated growth was also observed with 10% and 3% WT-MSC although less pronounced ($P = 0.4$ and 0.55, respectively). No differences in tumour size were observed between *DsRed*-DLD-1 xenografts mixed with untransduced MSC and xenografts mixed with *GFP*-MSC (data not shown).

Taken together, these results show that in this mixed xenograft model, a substantial proportion of *TRAIL*-MSC within the tumour was necessary for inhibition of tumour growth. Additionally, WT-MSC were able to support DLD-1 xenograft growth in this model depending on their frequency within the tumour.

Discussion

Our study on lentiviral *TRAIL*-transgenic human MSC yielded the following novel results: (1) *TRAIL*-MSC maintained their MSC characteristics without malignant transformation. (2) *TRAIL*-MSC could induce apoptosis in interacting CRC cells resulting in growth inhibition of TRAIL-sensitive CRC cells as well as of two CRC-cell lines resistant to soluble TRAIL. (3) However, a substantial intratumoral proportion of *TRAIL*-MSC was required to yield such anti-tumour effect *in vivo* and the anti-tumour effect of systemically applied *TRAIL*-MSC was hampered by their low rate of tumour integration. (4) WT-MSC exerted a tumour growth-supporting effect in CRC xenografts.

Our study originated from the reported TRAIL sensitivity of selected CRC-cell lines and our observation of a resistance of human MSC to soluble TRAIL. In our work on the sensitivity of MSC and CRC cells to soluble TRAIL we choose a concentration of 100 ng/ml soluble TRAIL. This represents 10% to 1% of the concentrations reached with recombinant TRAIL in clinical studies [28] but is comparable to doses used in other *in vitro* studies [13]. As further dose escalation does not result in altered response [13, 29] the results obtained in our study are regarded representative for the assessment of TRAIL sensitivity.

We show that transduction of human MSC with a third generation lentiviral construct comprising a self-inactivating 3′LTR and the cDNA of *TRAIL* does not change defining MSC characteristics. Interestingly, transgenic *TRAIL* did not exert pro-apoptotic effects on MSC. An explanation consists of a low sensitivity of MSC for TRAIL as described for other non-malignant cells. Importantly, no signs of malignant transformation were observed for lentivirally transduced MSC *in vitro* and *in vivo*.

Based on our data we suggest that the lasting transmembraneous expression of TRAIL in *TRAIL*-MSC is essential for a relevant anti-tumour activity. Further research is warranted to evaluate whether a higher level of expression may facilitate clinical applications.

The four CRC-cell lines used in our study could be divided in lines sensitive and resistant to soluble TRAIL. Strikingly, our data show that *TRAIL*-MSC could overcome resistance to soluble TRAIL in two specific cell lines through induction of apoptosis. This observation may be explained by direct cell–cell contact which might either exert higher persistent concentrations of TRAIL or additional pro-apoptotic inter-cellular communications compared to short-lived soluble TRAIL.

A recent work [15] reported anti-tumour activity of MSC-expressed trimeric TRAIL (stTRAIL). This secreted form of TRAIL could result in a broader radius of action within the tumour compared to membrane-expressed TRAIL. It would be interesting whether stTRAIL could help to overcome resistance to soluble TRAIL in our CRC cell model.

MSC with transgenic expression of anti-tumour genes have the potential to exert a strong inhibitory effect on tumour growth (reviewed in [2–4]) in models of systemic application [7, 30], in mixed s.c. xenografts [6] or by intratumoral injection [17]. In our view the systemic application of MSC as well as the mixed s.c. xenograft is better suited than intratumoral injection as the latter entails local mechanical damage probably skewing the results. Albeit we observed a strong effect in mixed xenografts, a systemic effect of *TRAIL*-MSC was not seen in our model. Our results suggest that this results from a limited integration of *TRAIL*-MSC into s.c. DLD-1-tumours due to their pulmonary entrapment. A pulmonary entrapment of systemically applied human MSC [31–34] but also of human tumour cells [35] has been reported. It has to be pointed out, that in most of those studies which demonstrated an anti-tumour effect of systemically applied transgenic MSC pulmonary tumour models were used [30, 36, 37]. Thus, such pulmonary entrapment of MSC may explain the increased anti-tumour effect of systemically applied transgenic MSC in

pulmonary tumour models compared to s.c. tumour models. However, tumour integration [7, 38, 39] and even proliferation [8] of systemically applied MSC was seen in s.c. tumours in a few studies. To date, no obvious explanation exists for these differential observations. The observed clinical effects of systemically applied MSC in patients [40–44] can be seen as an indication that a pulmonary entrapment as observed in mice may not be relevant in human beings. This raises the question whether further animal studies will help to clarify the relevance of pulmonary entrapment of MSC in human beings. Our data point out that the net effect of tumour-integrated MSC may depend on their frequency within the tumour. The results in our DLD-1 model suggest that a proportion of *TRAIL*-MSC exceeding 3% of total tumour cells may be relevant.

For native/WT-MSC we observed a supportive effect on tumour growth in our model of DLD-1 xenografts. Whether this is representative or just reflects a cell line-specific effect remains open. Similar observations have been reported previously in other cell models [38, 45–47] and also specifically for CRC-cell lines [48].

Taken together, our results suggest that *TRAIL*-MSC generated by lentiviral gene transfer may provide a safe approach for a novel anti-tumour therapy in CRC. However, a relevant anti-tumour activity may require a substantial intratumoral presence of transplanted *TRAIL*-MSC and has to be weighted against a potential tumour growth-supporting effect of MSC. Thus, our study warrants further investigation on the use of *TRAIL*-MSC as vehicles of tumour therapy perspectively including pilot clinical trials.

Acknowledgements

We are grateful to the donors who gave consent for the use of their bone marrow aspirates. We thank D. Wand, Ph.D., Department of Human Genetics, Medical Faculty of the Martin-Luther-University Halle-Wittenberg for performing the karyotype analysis. The study was supported in part by grants from the Federal State of Saxonia-Anhalt and the German Ministry of Education and Research through the Wilhelm-Roux-Program at the Medical Faculty of the Martin-Luther-University Halle-Wittenberg (1/09 3/15 6/08, 3/27) (L.P.M.) and the European Union through BioService Halle GmbH (J.L.).

Declaration of interest

None of the authors has to declare a commercial interest related to the contents of the study.

References

1. **Wolpin BM, Mayer RJ.** Systemic treatment of colorectal cancer. *Gastroenterology.* 2008; 134: 1296–310.
2. **Aboody KS, Najbauer J, Danks MK.** Stem and progenitor cell-mediated tumor selective gene therapy. *Gene Ther.* 2008; 15: 739–52.
3. **Corsten MF, Shah K.** Therapeutic stem-cells for cancer treatment: hopes and hurdles in tactical warfare. *Lancet Oncol.* 2008; 9: 376–84.
4. **Lazennec G, Jorgensen C.** Concise review: adult multipotent stromal cells and cancer: risk or benefit? *Stem Cells.* 2008; 26: 1387–94.
5. **Dominici M, Le Blanc K, Mueller I, *et al.*** Minimal criteria for defining multipotent mesenchymal stromal cells. The International Society for Cellular Therapy position statement. *Cytotherapy.* 2006; 8: 315–7.
6. **Studeny M, Marini FC, Champlin RE *et al.*** Bone marrow-derived mesenchymal stem cells as vehicles for interferon- beta delivery into tumors. *Cancer Res.* 2002; 62: 3603–8.
7. **Kucerova L, Altanerova V, Matuskova M *et al.*** Adipose tissue-derived human mesenchymal stem cells mediated prodrug cancer gene therapy. *Cancer Res.* 2007; 67: 6304–13.
8. **Hung SC, Deng WP, Yang WK *et al.*** Mesenchymal stem cell targeting of microscopic tumors and tumor stroma development monitored by noninvasive *in vivo* positron emission tomography imaging. *Clin Cancer Res.* 2005; 11: 7749–56.
9. **Nauta AJ, Fibbe WE.** Immunomodulatory properties of mesenchymal stromal cells. *Blood.* 2007; 110: 3499–506.
10. **Mueller LP, Luetzkendorf J, Mueller T *et al.*** Presence of mesenchymal stem cells in human bone marrow after exposure to chemotherapy: evidence of resistance to apoptosis induction. *Stem Cells.* 2006; 24: 2753–65.
11. **Almasan A, Ashkenazi A.** Apo2L/TRAIL: apoptosis signaling, biology, and potential for cancer therapy. *Cytokine Growth Factor Rev.* 2003; 14: 337–48.
12. **Ashkenazi A, Herbst RS.** To kill a tumor cell: the potential of proapoptotic receptor agonists. *J Clin Invest.* 2008; 118: 1979–90.
13. **Galligan L, Longley DB, McEwan M *et al.*** Chemotherapy and TRAIL-mediated colon cancer cell death: the roles of p53, TRAIL receptors, and c-FLIP. *Mol Cancer Ther.* 2005; 4: 2026–36.
14. **van Geelen CM, de Vries EG, Le TK *et al.*** Differential modulation of the TRAIL receptors and the CD95 receptor in colon carcinoma cell lines. *Br J Cancer.* 2003; 89: 363–73.
15. **Kim SM, Lim JY, Park SI *et al.*** Gene therapy using TRAIL-secreting human umbilical cord blood-derived mesenchymal stem cells against intracranial glioma. *Cancer Res.* 2008; 68: 9614–23.
16. **Ehtesham M, Kabos P, Gutierrez MA *et al.*** Induction of glioblastoma apoptosis using neural stem cell-mediated delivery of tumor necrosis factor-related apoptosis-inducing ligand. *Cancer Res.* 2002; 62: 7170–4.
17. **Mohr A, Lyons M, Deedigan L *et al.*** Mesenchymal stem cells expressing TRAIL lead to tumour growth inhibition in an experimental lung cancer model. *J Cell Mol Med.* 2008; 12: 2628–43.
18. **Shah K, Bureau E, Kim DE *et al.*** Glioma therapy and real-time imaging of neural precursor cell migration and tumor regression. *Ann Neurol.* 2005; 57: 34–41.
19. **Haleem-Smith H, Derfoul A, Okafor C *et al.*** Optimization of high-efficiency transfection of adult human mesenchymal stem cells *in vitro*. *Mol Biotechnol.* 2005; 30: 9–20.
20. **Larson BL, Ylostalo J, Prockop DJ.** Human multipotent stromal cells undergo

sharp transition from division to development in culture. *Stem Cells.* 2008; 26: 193–201.

21. **Chan J, O'Donoghue K, de la Fuente J *et al.*** Human fetal mesenchymal stem cells as vehicles for gene delivery. *Stem Cells.* 2005; 23: 93–102.
22. **Dull T, Zufferey R, Kelly M *et al.*** A third-generation lentivirus vector with a conditional packaging system. *J Virol.* 1998; 72: 8463–71.
23. **Skehan P, Storeng R, Scudiero D *et al.*** New colorimetric cytotoxicity assay for anticancer-drug screening. *J Natl Cancer Inst.* 1990; 82: 1107–12.
24. **Lois C, Hong EJ, Pease S *et al.*** Germline transmission and tissue-specific expression of transgenes delivered by lentiviral vectors. *Science.* 2002; 295: 868–72.
25. **Mueller T, Voigt W, Simon H *et al.*** Failure of activation of caspase-9 induces a higher threshold for apoptosis and cisplatin resistance in testicular cancer. *Cancer Res.* 2003; 63: 513–21.
26. **Zhang L, Gu J, Lin T *et al.*** Mechanisms involved in development of resistance to adenovirus-mediated proapoptotic gene therapy in DLD1 human colon cancer cell line. *Gene Ther.* 2002; 9: 1262–70.
27. **Moss DK, Lane JD.** Microtubules: orgotten players in the apoptotic execution phase. *Trends Cell Biol.* 2006; 16: 330–8.
28. **Ling J, Herbst RS, Mendelson DS *et al.*** Apo2L/TRAIL pharmacokinetics in a phase 1a trial in advanced cancer and lymphoma. *J Clin Oncol (Meeting Abstracts).* 2006; 24: 3047.
29. **Ashkenazi A, Pai RC, Fong S *et al.*** Safety and antitumor activity of recombinant soluble Apo2 ligand. *J Clin Invest.* 1999; 104: 155–62.
30. **Studeny M, Marini FC, Dembinski JL *et al.*** Mesenchymal stem cells: potential precursors for tumor stroma and targeted-delivery vehicles for anticancer agents. *J Natl Cancer Inst.* 2004; 96: 1593–603.
31. **Barbash IM, Chouraqui P, Baron J *et al.*** Systemic delivery of bone marrow-derived mesenchymal stem cells to the infarcted myocardium: feasibility, cell migration, and body distribution. *Circulation.* 2003; 108: 863–8.
32. **Bentzon JF, Stenderup K, Hansen FD *et al.*** Tissue distribution and engraftment of human mesenchymal stem cells immortalized by human telomerase reverse transcriptase gene. *Biochem Biophys Res Commun.* 2005; 330: 633–40.
33. **Gao J, Dennis JE, Muzic RF *et al.*** The dynamic *in vivo* distribution of bone marrow-derived mesenchymal stem cells after infusion. *Cells Tissues Organs.* 2001; 169: 12–20.
34. **Hakkarainen T, Sarkioja M, Lehenkari P *et al.*** Human mesenchymal stem cells lack tumor tropism but enhance the antitumor activity of oncolytic adenoviruses in orthotopic lung and breast tumors. *Hum Gene Ther.* 2007; 18: 627–41.
35. **Power AT, Bell JC.** Cell-based delivery of oncolytic viruses: a new strategic alliance for a biological strike against cancer. *Mol Ther.* 2007; 15: 660–5.
36. **Stoff-Khalili MA, Rivera AA, Mathis JM *et al.*** Mesenchymal stem cells as a vehicle for targeted delivery of CRAds to lung metastases of breast carcinoma. *Breast Cancer Res Treat.* 2007; 105: 157–67.
37. **Kanehira M, Xin H, Hoshino K *et al.*** Targeted delivery of NK4 to multiple lung tumors by bone marrow-derived mesenchymal stem cells. *Cancer Gene Ther.* 2007; 14: 894–903.
38. **Karnoub AE, Dash AB, Vo AP *et al.*** Mesenchymal stem cells within tumour stroma promote breast cancer metastasis. *Nature.* 2007; 449: 557–63.
39. **Khakoo AY, Pati S, Anderson SA *et al.*** Human mesenchymal stem cells exert potent antitumorigenic effects in a model of Kaposi's sarcoma. *J Exp Med.* 2006; 203: 1235–47.
40. **Christopeit M, Schendel M, Foll J *et al.*** Marked improvement of severe progressive systemic sclerosis after transplantation of mesenchymal stem cells from an allogeneic haploidentical-related donor mediated by ligation of CD137L. *Leukemia.* 2008; 22: 1062–4.
41. **Horwitz EM, Gordon PL, Koo WK *et al.*** Isolated allogeneic bone marrow-derived mesenchymal cells engraft and stimulate growth in children with osteogenesis imperfecta: Implications for cell therapy of bone. *Proc Natl Acad Sci USA.* 2002; 99: 8932–7.
42. **Koc ON, Day J, Nieder M *et al.*** Allogeneic mesenchymal stem cell infusion for treatment of metachromatic leukodystrophy (MLD) and Hurler syndrome (MPS-IH). *Bone Marrow Transplant.* 2002; 30: 215–22.
43. **Lazarus HM, Koc ON, Devine SM *et al.*** Cotransplantation of HLA-identical sibling culture-expanded mesenchymal stem cells and hematopoietic stem cells in hematologic malignancy patients. *Biol Blood Marrow Transplant.* 2005; 11: 389–98.
44. **Le Blanc K, Frassoni F, Ball L *et al.*** Mesenchymal stem cells for treatment of steroid-resistant, severe, acute graft-*versus*-host disease: a phase II study. *Lancet.* 2008; 371: 1579–86.
45. **Djouad F, Bony C, Apparailly F *et al.*** Earlier onset of syngeneic tumors in the presence of mesenchymal stem cells. *Transplantation.* 2006; 82: 1060–6.
46. **Ramasamy R, Lam EW, Soeiro I *et al.*** Mesenchymal stem cells inhibit proliferation and apoptosis of tumor cells: impact on *in vivo* tumor growth. *Leukemia.* 2007; 21: 304–10.
47. **Yu JM, Jun ES, Bae YC *et al.*** Mesenchymal stem cells derived from human adipose tissues favor tumor cell growth *in vivo*. *Stem Cells and Development.* 2008; 17: 463–73.
48. **Zhu W, Xu W, Jiang R *et al.*** Mesenchymal stem cells derived from bone marrow favor tumor cell growth *in vivo*. *Exp Mol Pathol.* 2006; 80: 267–74.